Robustness of 40 Gb/s ASK modulation formats in the practical system infrastructure

Erwan Pincemin, Antoine Tan, Aude Bezard

France Telecom, Research & Development Division, Technopôle Anticipa, 2 Avenue Pierre Marzin,
22307 Lannion Cedex, France
Tel: +33 (0)2 96 05 06 59, Fax: +33 (0)2 96 05 12 52
erwan.pincemin@francetelecom.com

Alessandro Tonello, Stefano Wabnitz

Laboratoire de Physique de l'Université de Bourgogne, UMR CNRS 5027, 9 Avenue Alain Savar
21078 Dijon, France
alessandro.tonello@u-bourgogne.fr

Juan Diego Ania-Castañón, Sergei Turitsyn

Photonics research group, School of Engineering and Applied Science, Aston University
Birmingham B4 7ET, UK
Tel: +33 (0)2 96 05 06 59, Fax: +33 (0)2 96 05 12 52
J.D.Ania-Castanon@aston.ac.uk

Abstract: In this work, we analyzed by means of numerical and laboratory experiments the resilience of 40 Gb/s amplitude shift keying modulation formats to transmission impairments in standard single-mode fiber lines as well as to optical filtering introduced by the optical add/drop multiplexer cascade. Our study is a pre-requisite to assess the implementation of cost-effective 40 Gb/s modulation technology in next generation high bit-rate robust optical transport networks.

©2006 Optical Society of America

OCIS codes: (060.4080) Modulation; (060.4510) Optical communications; (190.4370) Nonlinear optics, fibers; (999.9999) Optical add/drop multiplexer.

_____

References and links

1. "Mintera achieves record ultra long haul transmission distance at 40 Gb/s", March 2002; "Migrating to 40-Gbit/sec DWDM networks," FibreSystems Europe, September 2002, http://www.mintera.com.
2. "Lucent Technologies ships its new, industry-leading optical system - LambdaXtreme™ transport - to Deutsche Telekom," Lucent press release, March 2002; "Lambdaxtreme™ Transport successfully completes field trial in Deutsche Telekom network," Lucent press release, July 2002, http:// www.lucent.com.
3. "MCI, Xtera, Mintera, and Juniper Networks Show High-Bandwidth Optical Technology Capable of Reaching Farther Distances over Existing Fiber Networks," FibreSystems Europe, December 2005, http://www.mintera.com.
4. "40G moves back onto the agenda," FibreSystems Europe, May 2004, http://www.strataligtht.com.
5. H. Bissessur, C. Bresson, J. Hébert, J.P. Soigné, R. Bouchenot, C. Bastide, M. Bénomar, A. Hugbart, S. Ruggeri, "Transmission of 40x43 Gb/s over 2540 km of SMF with terrestrial 100-km spans using NRZ format," in *Optical Fiber Communication Conference*, Technical Digest (Optical Society of America, 2003), paper FN3.
6. A.H Gnauck, X. Liu, X. Wei, D.M. Gill, E.C. Burrows, "Comparison of modulation format for 42.7 Gbit/s single-channel transmission through 1980 km of SSMF," IEEE Photon. Technol. Lett. **16**, 909-911 (2004).
7. D.F. Grosz, A. Agarwal, S. Banerjee, D.N. Maywar, A.P. Küng, "All-Raman Ultralong-haul single-wideband DWDM transmission systems with OADM capability," J. Lightwave Technol. **22**, 423-432 (2004).

8. A. H. Gnauck, P. J. Winzer , S. Chandrasekhar Hybrid 10/40-G Transmission on a 50-GHz Grid Through 2800 km of SSMF and Seven Optical Add–Drops," IEEE Photon. Technol. Lett. **17**, 2203-2205 (2005).
9. CS-TDCM tuneable dispersion compensation module data sheet, http://www.teraxion.com.
10. M. O'Sullivan, "Electronic dispersion compensation technique for optical communication systems," in *Proeedings ECOC 2005*, Glasgow, Scotland, 2005, paper Tu3.2.1.
    J.P. Elbers, H. Wernz, H. Griesser, C. Glingener, A. Faerbert, S. Langenbach, N. Stojanovic, C. Dorschky, T. Kupfer, C. Schulien, "Measurement of the dispersion tolerance of optical duobinary with an MLSE receiver at 10.7 Gb/s," in *Proceedings OFC 2005*, CA, USA, 2005, paper OThJ4.
11. G. Charlet, P. Tran, H. Mardoyan, M. Lefrançois, T. Fauconnier, S. Bigo,"151x43 Gbit/s Transmission over 4880 km based on RZ-DQPSK," in *Proc. ECOC 2005*, Glasgow, Scotland, 2005, paper Th4.1.4.
12. Specialty photonics products overview, Rightwave EWBDK-C data sheet, http://www.ofs.dk.
13. E. Pincemin, D. Grot, C. Borsier, J.D. Ania-Castañón, S.K. Turitsyn, "Impact of the fiber type and dispersion management on the performance of an NRZ 16x40 Gbit/s DWDM transmission system," IEEE Photon. Technol. Lett. **16**, 2362-2364 (2004).
14. A. Mecozzi, C.B. Clausen, M. Shtaif, S. G. Park, A. H. Gnauck, "Cancellation of timing and amplitude jitter in symmetric links using highly dispersed pulses," IEEE Photon. Technol. Lett. **13**, 445-447 (2001).
15. W. Idler, A. Klekamp, R. Dischler, "System performance and tolerances of 43 DPSK modulation formats," in *Proceedings ECOC 2003*, Rimini, Italy, 2003, paper Th2.6.3.
16. A. Klekamp, R. Dischler, W. Idler, "Impairments of bit-to-bit alternate-polarization on non-linear threshold, CD and DGD tolerance of 43 Gbit/s ASK and DPSK formats," in *Optical Fiber Communication Conference and Exposition and The National Fiber Optic Engineers Conference*, Technical Digest (CD) (Optical Society of America, 2005), paper OFN3.
17. R. Dischler, A. Klekamp, J. Lazaro, W. Idler, "Experimental comparison of non linear threshold and optimum pre dispersion of 43 Gbit/s ASK and DPSK formats," in *Optical Fiber Communication Conference*, Technical Digest (CD) (Optical Society of America, 2004), paper TuF4.
18. A. Klekamp, R. Dischler, W. Idler, "A comparison of 43 Gbit/s ASK and DPSK modulation formats regarding system performance and tolerances," in *Proceedings ITG Fachtagung Photonische Netze*, Germany, 2005, paper 26.
19. F. An, M. Marhic, L. Kazovsky, Y. Akasaka, D. Harris, R. Huang, "Comparison of linear fiber impairments tolerance among 40 Gbit/s modulation formats," in *Optical Fiber Communication Conference*, Technical Digest (Optical Society of America, 2003), paper FE2.
20. P. Pecci, S. Lanne, Y. Frignac, J.C. Antona, G. Charlet, S. Bigo, "Tolerance to dispersion compensation parameters of six modulation formats in systems operating at 43 Gbit/s," Electron. Lett. **39**, 1844-1846 (2003).
21. XPRV2021 data sheet, http://www.u2t.de; DSCR404 data sheet, http://www.chipsat.com.
22. G. Castañón, O. Vassilieva, S. Choudhary, T. Hoshida, "Requirements of filter characteristics for 40 Gbit/s-based DWDM systems," in *Proceedings ECOC 2001*, Amsterdam, Nederlands, 2001, paper Mo.F.3.5.
23. A. Hodzic, M. Winter,, B. Konrad, S. Randel, K. Petermann, "Optimized filtering for 40-Gbit/s/ch-based DWDM transmission systems over standard single-mode fiber," IEEE Photon. Technol. Lett. **15**, 1002-1004 (2003).
24. G. Bosco, A. Carena, V. Curri,; R. Gaudino, P. Poggiolini, "On the use of NRZ, RZ, and CSRZ modulation at 40 Gbit/s with narrow DWDM channel spacing," J. Lightwave Technol., **20**, No.9, pp 1694-1704 (2002).
25. C. Xie, L. Möller, H. Haunstein, S. Hunsche, "Comparison of system tolerance to polarization mode dispersion between different modulation formats," IEEE Photon. Technol. Lett.**15**, 1168-1170 (2003).
26. A.H. Gnauck, P. Winzer, S. Chandrasekhar, "Hybrid 10/40 G transmission on a 50-GHz ITU grid through 2800 km of SSMF and seven optical add-drops," IEEE Photon. Technol. Lett. **17**, 2203-2205 (2005).
27. A. H. Gnauck, P. J.Winzer, S. Chandrasekhar, and C. Dorrer, "Spectrally efficient (0.8 b/s/Hz) 1-Tb/s (25_42.7 Gb/s) RZ-DQPSK transmission over 28 100-km SSMF spans with 7 optical add/drops," in *Proceedings ECOC 2004*, Stockholm, Sweden, 2004, Postdeadline paper Th4.4.1.
28. A. Agarwal, S. Banerjee, D. F. Grosz, A. P. Kung, D. N. Maywar, and T. H.Wood, "Ultralong-haul transmission of 40-Gb/s RZ-DPSK in a 10/40 G hybrid system over 2500 km of NZ-DSF," IEEE Photon. Technol. Lett. **15**, 1779–1781 (2003).

_____

1. Introduction

The recent downturn of the telecommunication industry has undoubtedly delayed the field deployment of 40 Gb/s transmission systems, whose first 40 Gb/s commercial products have been available since 2002 [1-2]. The present renewed interest in 40 Gb/s technology has been eased by advances in the technology of transponders, and hinges on the promise of capital

expenditure reductions for wavelength-division multiplexed (*WDM*) long-haul and metropolitan transmission systems [3-4]. Such systems are expected to satisfy the practical requirements of the existing carriers' fiber infrastructure, and the constraints imposed by typical functionalities of next generation all-optical networks. Critical issues remain system compatibility with standard single mode fiber (*SSMF*) lines [5-6] (which are frequently hampered by relatively large polarisation mode dispersion) and optical add/drop (*OADM*) capabilities [7-8]. To this end, special enabling technologies may be adopted, such as modulation formats resilient to transmission impairments and *OADM* filtering, distributed Raman amplification (*DRA*), and dynamic channel equalization [9-10]. In this context, it is crucial to combine the efforts of the optical research community and of operators, in order to guide the practical implementation of new high-speed optical communication technologies.

The actual deployment conditions of a 40 Gb/s transmission system are generally quite different from quasi-ideal laboratory conditions. Therefore in this work we intend to investigate the role of key practical constraints that may lead to serious obstacles to the successful introduction of 40 Gb/s *WDM EDFA*-based transmission systems. In particular, we aim at comparing the robustness of different modulation formats, when coping with such constraints. We do not aim to present in this paper an ultimate solution to 40 Gb/s system design. Our purpose is to pinpoint the various steps to be simultaneously addressed by carriers so that they can be aware of possible blocking issues in their deployment of 40 Gb/s systems on their metropolitan and/or core transport networks. Clearly, the proper understanding of practical constraints is also of concern for the optical research community. We believe that our analysis is going to provide timely and important guidelines in this rapidly advancing field.

In this work we will investigate by means of both laboratory and simulation experiments the transmission robustness of different 40 Gb/s amplitude shift keying (*ASK*) modulation formats. Namely, non-return-to-zero (*NRZ*), 33% return-to-zero (*33% RZ*) and carrier-suppressed return-to-zero (*CS-RZ*). The transmission quality of the optical signals is subject to the following impairments: optical signal-to-noise ratio (*OSNR*) degradation, intra-channel nonlinearities, residual chromatic dispersion (*CD*), first-order polarisation mode dispersion (*PMD*) and optical filtering at the add/drop sites. In our study, we select the experimental configurations which closely reflect practical conditions of existing terrestrial fiber link infrastructures. In contrast with previous laboratory transmission experiments which often used non-zero dispersion shifted fiber (*NZDSF*) links, we will only consider in our investigations the case of a *SSMF*-based link, which is the most largely deployed fiber on terrestrial transmission networks of historical European carriers. In addition, we are going to employ Erbium-doped fiber amplifiers (*EDFA*) without any Raman amplification. Clearly, from the research viewpoint it is important to carry out comprehensive investigations of the performance improvements introduced by distributed Raman amplifiers (DRA). However, the potential advantages offered by DRA should be weighted alongside with practical issues of importance for operators, that may ultimately hamper deployment of DRA systems. Namely: (a) The need for carriers to measure fiber losses at Raman pump wavelengths (before the installation of the transmission system); (b) The uncertain reliability of optical connectors located between Raman pumps and fiber spans (involving system outage in case of failure); (c) The ocular safety of people in charge of maintenance (because of the presence of high optical powers in the system). Finally, reflecting the practical conditions of fiber links, in our experiments we did not introduce a precise optimization of the dispersion map. As a result, the residual dispersion per span was not accurately tuned to a predefined optimal value.

2. Experimental set-up

In Fig. 1 we illustrate our experimental setup. The transmitter was composed of sixteen *DFB* laser sources, ranging from 1544.53 to 1556.56 nm on a 100-GHz *ITU* grid. Odd and even channels were separately multiplexed and modulated using independent sets of two in-series LiNbO$_3$ modulators, equipped with automatic bias control (*ABC*) loop circuits. The task of

these circuits is the stabilization of the correct working point of LiNbO$_3$ modulators. This is achieved by means of continuously and automatically changing the modulator bias voltage, in order to keep track of the natural drift of the modulator transmission transfer function.
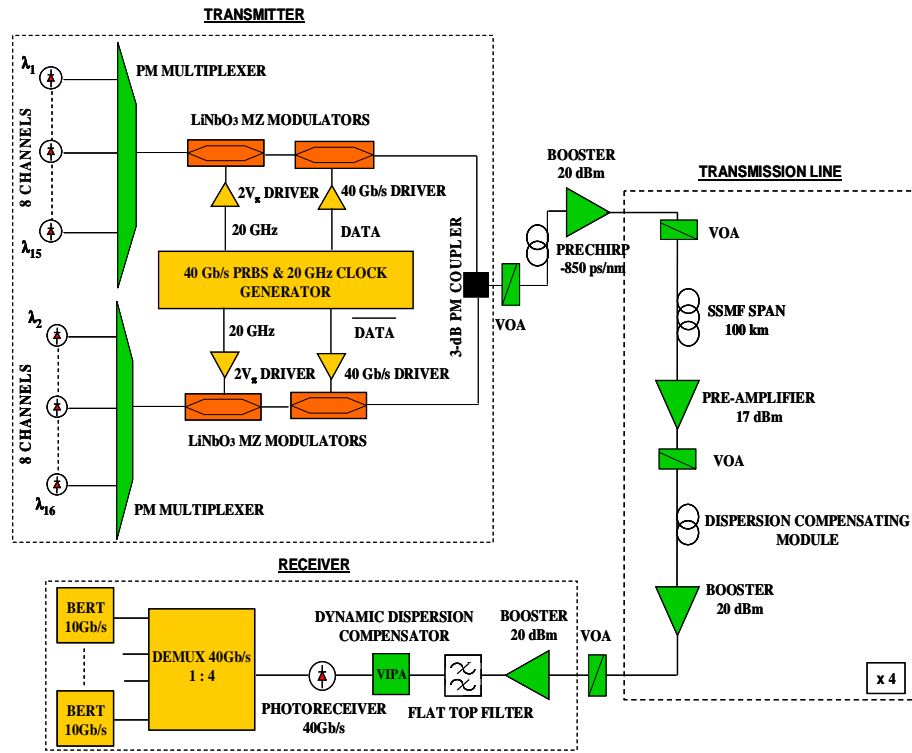

Fig 1. Schematic of the experimental set-up.

The first modulators (the pulse carvers) were driven at 20 GHz with a 2V$_\pi$ clock and polarized at the null (maximum) transmission point when the *CS-RZ* (*33% RZ*) format was generated. Each of the second set of modulators was driven by uncorrelated 40 Gb/s 2^{31}-1 pseudo-random bit sequences (*PRBS*), obtained by electrically interleaving four delayed copies of 10 Gbit/s 2^{31}-1 *PRBS*. Switching off the *RZ* drivers, while polarizing the pulse carvers to their maximum transmission point, has permitted us to generate the *NRZ* format. Odd and even wavelengths were recombined through a polarisation maintaining 3-dB coupler, so that we could preserve co-polarized channels. In Fig. 2 we show a temporal and spectral characterization of our transmitter for the three modulation formats under test. We measured the extinction ratios of the *NRZ*, *CS-RZ* and *33% RZ* formats by means of a Tektronix *CSA8200* oscilloscope and a *80C10* optical sampling module equipped with a 65 GHz photodiode. These measurements led to extinction ratios of 12.6, 14.1 and 15.3 dB respectively, as indicated on the scope screens of Fig. 2.
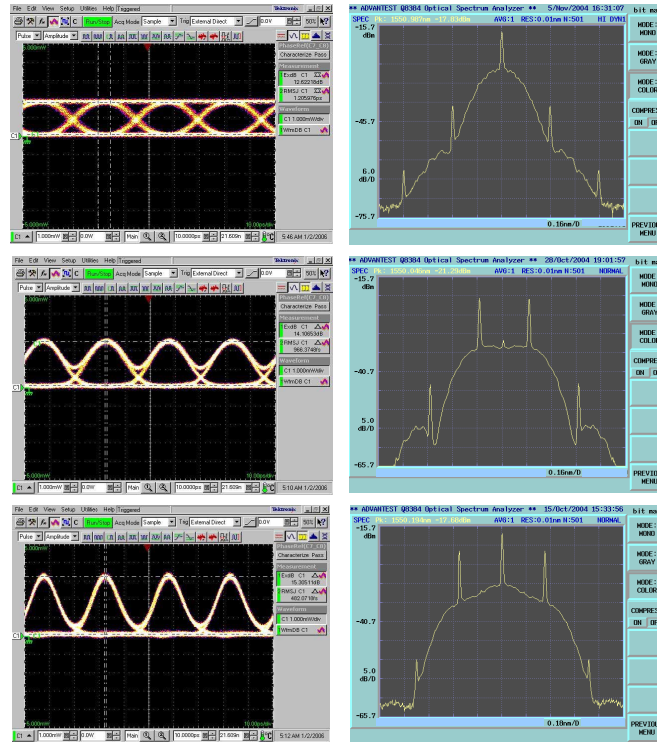
Fig. 2. Temporal and spectral characterization of our transmitters: *NRZ* (top), *CS-RZ* (middle), *33% RZ* (bottom).

We have started our study by evaluating the resilience of modulation formats to intrachannel nonlinear effects. We used a straight transmission line constituted by four distinct 100-km spans of *SSMF*. Our presumption is that *ASK* formats, in spite of their reduced robustness to *PMD* with respect to *DQPSK* modulations for example [11], will be the formats of choice for the deployment of 40 Gb/s systems in moderate length transmission lines, namely for metropolitan and long-haul applications (not for ultra long-haul ones). This motivates our choice of a relatively short link consisting of 4x100 km spans. The cumulated dispersion and slope of *SSMF* were compensated by dispersion compensation modules tailored for compensating 100-km *SSMF* spans (*DCM-100)*. Note that our commercial *DCM* have a tolerance of ± 2% [12] of their cumulated dispersion. This translates in a cumulated dispersion in the range [-1665,-1735] ps/nm for the *DCM-100* that were used in our experiment. To reproduce practical field conditions, the residual dispersion per span was not precisely tuned (by adding for example small pieces of *SSMF* which would allow for reaching a certain target for the span compensation). Our resulting dispersion map for the channel at 1550.12 nm is shown in Fig. 4, where we can observe a compensation ratio per span which varies between 97.9 % and 98.5 %. Fiber span (~ 21 dB) and *DCM* (~ 10 dB) losses were compensated by double stage *EDFAs* with a global noise figure of 5.5 dB. The optical power injected into the *DCM* was fixed to -2 dBm per channel. We reduced the impact of nonlinearities, in particular intra-channel cross-phase modulation (*IXPM*) and four-wave mixing (*IFWM*), by including a -850 ps/nm prechirp at 1550.12 nm. This leads to an initial pulse broadening and a symmetric dispersion map [13-14], whereby the first (second) half of span propagation was in the negative (positive) cumulated dispersion regime. We selected the measured channel at the receiver with a *XTRACT*^{TM} wavelength/bandwidth tuneable square flat-top optical filter. The amplitude and group delay transfer function of our receiver optical

filter are shown on Fig. 3 (blue curves). At the transmission end, the residual dispersion was adjusted by a virtually-imaged phased-array (*VIPA*) dispersion compensator (with a nominal dispersion of about +100 ps/nm) in order to optimize the bit-error-rate (*BER*) of 10 Gbit/s tributaries after 1:4 electrical demultiplexing.
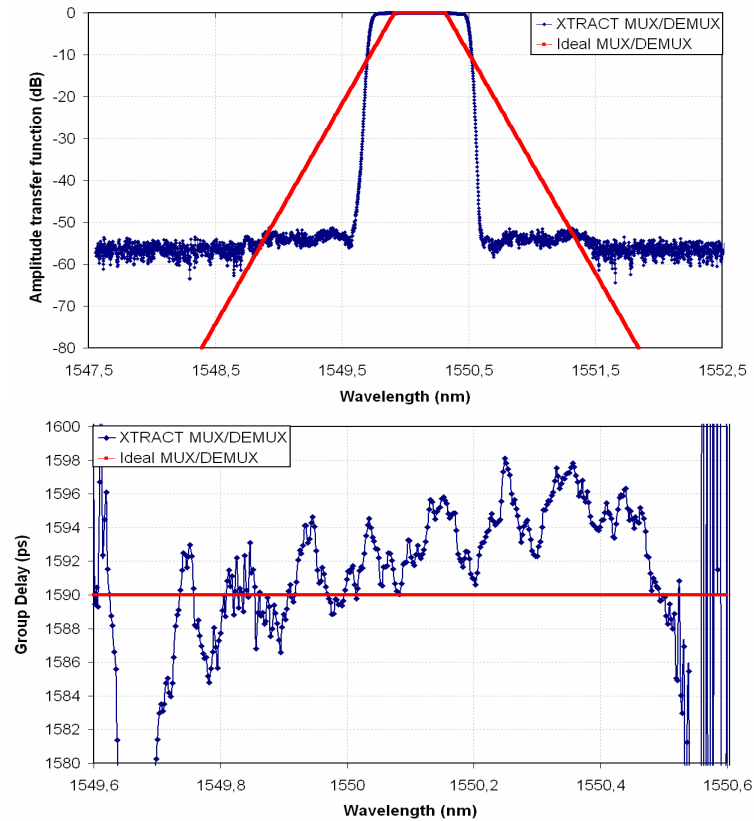

Fig. 3. Amplitude and group delay transfer function of the *XTRACT*^{TM} square flat-top optical filter used in the receiver (blue curves) and of an ideal 100 GHz flat-top demultiplexer (red curves).

3. Simulation results

In order to guide our experiments, we reproduced the above discussed experimental setup by numerically solving the nonlinear Schrödinger equation with a split-step Fourier algorithm by the means of a commercial system simulation software package (*VPI Transmission Maker*^{TM}) using 2048-long pseudo-random bit sequences. Figure 5 shows our simulation results that compare the transmission performance of the *NRZ*, *33% RZ* and *CS-RZ* modulation formats. We show the contour level plots of *Q*-factor values (in dB) for the central channel out of a comb of five simulated channels with a channel separation of 200 GHz (to neglect the impact of inter-channel nonlinearities). Figure 5 illustrates the dependence of the *Q*-factor at the output of the 4x100 km spans of *SSMF* as a function of both the prechirp and the launch signal average power (P_S). Note that for each prechirp value, we optimized the postchirp in order to obtain the highest possible Q value. For simplicity, we considered a flat-top optical filter with the same bandwidth value of 100 GHz for all formats (in contrast with the experiments where the filter bandwidth was optimized for each modulation format). The dispersion map that was used in the simulations is identical to the actual map of our experiments (see Fig. 4).
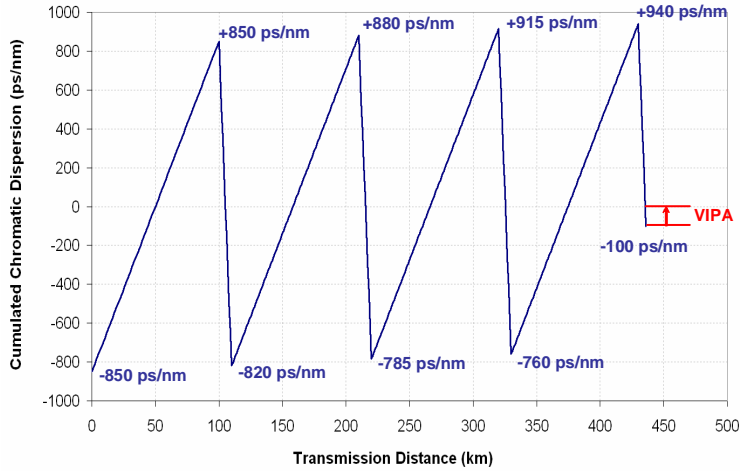
Fig. 4. Dispersion map used in the experiment for the channel at 1550.12 nm.
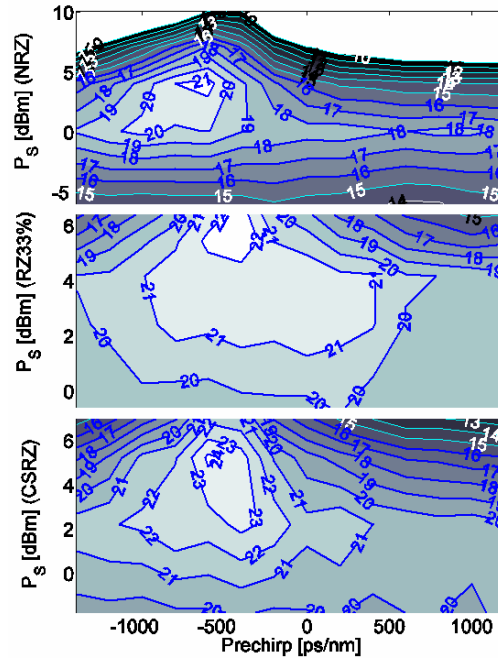

Fig. 5. Numerical simulation of *Q*-factor levels (in dB) vs. prechirp and signal average power (P_S), for *NRZ* (top), *33% RZ* (middle) and *CS-RZ* (bottom) formats with 200 GHz channel spacing. Postchirp is adjusted for each prechirp value to obtain best performance.

As can be seen in Fig. 5, whenever the launch signal power has a relatively low value, for all modulation formats the selection of a particular prechirp is not critical for system performance. On the other hand, as the input power of the signal P_S increases above 1 dBm, best performance is obtained for negative values of the prechirp. The optimal prechirp is equal to -500, -600 and -700 ps/nm for *33% RZ*, *CS-RZ* and *NRZ*, respectively. The results of Fig. 5 predict as well that, for well-spaced (200 GHz) channels, the *CS-RZ* format leads to about 2 dB performance improvement (in terms of *Q*-factor) over *NRZ* format and about 1 dB improvement over the *33% RZ* format.

4. Experimental results and discussion

In order to evaluate the robustness to intra-channel nonlinearities [5-6, 13, 15-18], we used only the 8 even channels with a spectral granularity of 200 GHz. In this configuration, inter-channel nonlinear effects can be neglected, while preserving the gain flatness of the *EDFA* as well as the proper operation of the *ABC* loop circuits (which require around 15 dBm of optical power for their stable operation). At the receiver, the 20-dB bandwidth of the *XTRACT*[TM] square flat-top optical filter was optimized for each format: it was fixed to nearly 0.7 nm for the *NRZ* and *CS-RZ* format*, and to 0.9 nm for the *33% RZ* format. The electrical 3-dB bandwidth of our receiver was fixed by its hardware: it consists of a 40-GHz *XPRV2021* u²t photoreceiver [21] connected to an electronic decision circuit and a 1:4 electrical demultiplexer. The dispersion map was kept unchanged throughout the measurements, while post-compensation at the receiver side was optimized for each format, by means of finely tuning, about its nominal value of +100 ps/nm, the extra dispersion that was introduced by the *VIPA* compensator.
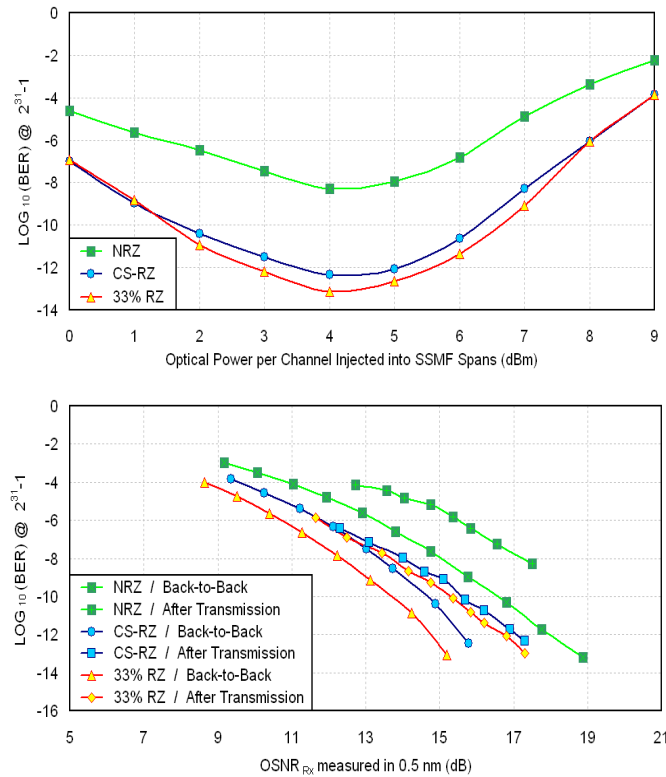
Fig. 6. *BER* versus power per channel injected into *SSMF* spans (top), *BER* versus the receiver *OSNR* in back-to-back and after transmission (bottom), for the central channel at 1550.12 nm.

Figure 6 (top) compares the *BER* of the central channel after transmission as a function of the channel power injected into *SSMF* spans. The input *OSNR* (measured in 0.5 nm) is equal to 25 dB. The optimal span input power (around 4 dBm) is virtually the same for all the modulation formats considered here. In contrast, the various modulation formats show different *BER* values at the optimum span input power: the *33% RZ* slightly outperforms the *CS-RZ*, and it is definitely better than the *NRZ* format. Nonetheless, in order to accurately evaluate the nonlinear penalty corresponding to each modulation format, it is important to measure as well the *BER* vs. *OSNR* at the receiver, as it is obtained both in back-to-back and

after 400-km transmission. These measurements were made at the optimum input power as we have previously determined. The superior resilience of *CS-RZ* to intra-channel nonlinearities is clear on the Fig. 6 (bottom). Indeed, for a *BER* of 10^{-9} the *OSNR* penalty is only 0.75 dB for *CS-RZ*, whereas it is 1.5 dB for *33% RZ*, and it is higher than 2 dB for *NRZ*. The 1 dB margin of the *33% RZ* in back-to-back *OSNR* sensitivity (when compared to *CS-RZ*) is erased after transmission owing to the larger sensitivity of this format to *IFWM*. The higher resilience of *CS-RZ* to this impairment is due to its relatively large duty cycle, as well as to its stronger pulse confinement (owing to the periodic π-phase shifts) which reduces pulse overlapping when chromatic dispersion accumulates. Figure 6 (bottom) also shows that *33% RZ* is the most resistant format to *OSNR* degradation: in back-to-back and for a *BER* of 10^{-9}, *33% RZ* has an *OSNR* margin of 0.75 (2.75) dB when compared to *CS-RZ* (*NRZ*).

Our present measurements of back-to-back sensitivities and resilience to intra-channel nonlinearities are globally in line with previous available results [6, 15-18]. It should be pointed out that we did not use *DRA* in our experiments, and for each format we optimized the optical filter bandwidth at the receiver.

Next we compared the modulation format resilience to residual *CD* and first order *PMD* or differential group delay (*DGD*) [15-16, 18-20]. Again we used the 8 even channels, and we kept fixed the previous tuning of the optical filter. *CD* increments were equal to +12.5 ps/nm in the range [-100, +100] ps/nm. The *DGD* was produced by means of a first-order *PMD* emulator. A polarization controller placed at its input permitted to ensure that the power splitting ratio between the two axes of the emulator was equal to 0.5 (corresponding to the worst case). The received *OSNR* for null *CD* or *DGD* was fixed in order to have a 10^{-9} *BER* independently of the modulation format. When varying the residual *CD* or *DGD*, *OSNR* penalties were measured by increasing the received *OSNR* up to a level where the received *BER* returned towards 10^{-9} (the *BER* value obtained at null *CD* or *DGD*).

Figure 7 (top) shows the *OSNR* penalty for each format vs. residual *CD* for the central channel. As can be seen, *NRZ* is most tolerant format to *CD* accumulation. For a 1 dB *OSNR* penalty, an acceptance window of 90, 75 and 60 ps/nm was observed for *NRZ*, *CS-RZ* and *33% RZ*, respectively. Clearly, the wider the pulse spectrum, the less resilient is the format to residual *CD*. Periodic π-phase alternation increases also *CD* resilience of *CS-RZ*, by reducing inter-symbol interference (*ISI*). Note that slight shifts observed on the *CD* curves against the 0 ps/nm point are due to the residual chirp of the emitter (in particular the pulse carvers). Figure 7 (bottom) shows the *OSNR* penalty for each format as a function of the *DGD*. With *33% RZ*, the accepted *DGD* (defined as the level of *DGD* that leads to 1 dB *OSNR* penalty) is maximal and equal to nearly 13 ps (it is 10.5 ps and 6.5 ps with the *CS-RZ* and *NRZ* formats, respectively). Clearly, the larger the pulse duty cycle, the lower is the modulation format robustness to *DGD*. In particular, when considering the *NRZ* format, the presence of *PMD* leads to a leaking of the "marks" energy into adjacent "spaces", which enhances the *BER*. The results shown in Fig. 8 explain well the inferior resilience of the *NRZ* format in comparison with the *33% RZ* format (the most robust facing *PMD*). Indeed, as shown by the plot at the right hand side of Fig. 8, the *33% RZ* format under the influence of 12 ps of *DGD* yields an eye diagram which is very close to what is obtained with the *NRZ* format with 0 ps of *DGD*. Finally note that the periodic π-phase shifts of the *CS-RZ* format do not affect the resilience of this format to *DGD*, unlike the case of *CD*.

Note that in these experiments we carried out a fine optimization of the output optical filter bandwidth, which in our opinion is important in order to ensure a fair comparison among the different formats when considering residual *CD* or *DGD* robustness.
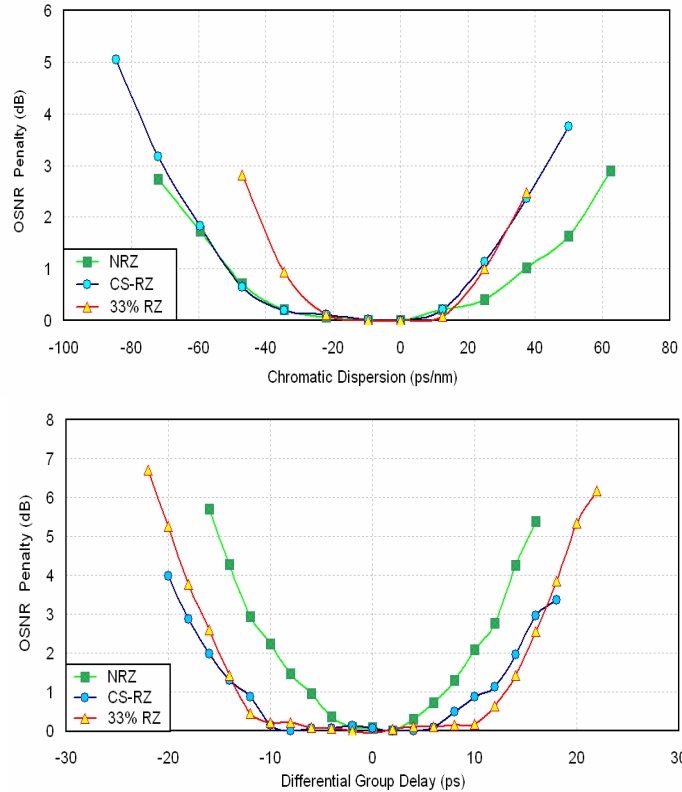
Fig. 7. *OSNR* penalty in 0.5 nm at fixed *BER*=10^{-9} versus residual *CD* (top), and *DGD* (bottom), for the central channel at 1550.12 nm.
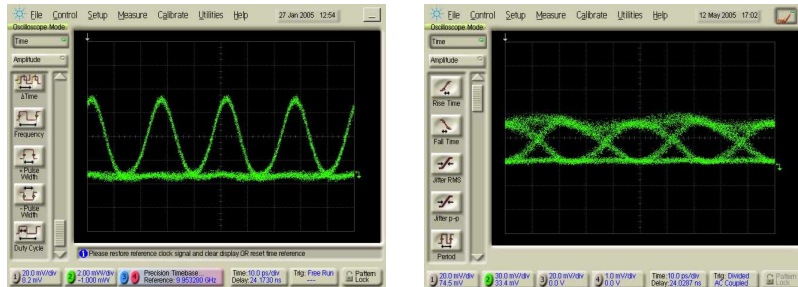

Fig. 8. Eye diagrams of the *33% RZ* modulation format when *DGD* is null (left hand side) and equal to 12 ps (right hand side).

Finally, in order to obtain a first assessment of the impact of an *OADM* cascade on the modulation format performance, we estimated the *ASK* formats resistance to changes of the output optical filter bandwidth and detuning [22-24]. We used the *XTRACT* square flat-top optical filter (as already mentioned in section 2), tuneable in wavelength and in bandwidth (on the range [200, 900] pm). In these measurements, we used all of the 16 channels spaced by 100 GHz, whereas the *OSNR* penalty was measured with respect to the reference *OSNR* obtained in the back-to-back case with the 8 even channels only and corresponding to a *BER* of 10^{-9}. Figure 9 (top) shows the *OSNR* penalty as a function of filter bandwidth. As expected, the *33% RZ* format is most impacted by output optical filtering, owing to its relatively large

spectral occupancy. At the optimum output filter bandwidth (~ 0.9 nm), the *OSNR* penalty for the *33% RZ* format is equal to 1.2 dB, and it grows significantly larger whenever the filter bandwidth is reduced below this optimal value. Whatever the modulation format under study, strong optical filtering indeed causes strong signal distortion: this fact, that can be detected in both the spectrum and the eye diagram, clearly degrades the system performance. On the opposite direction, penalties grow also as the optical filter bandwidth is increased. This is due to the imperfect rejection of crosstalk from neighbouring channels. Fig. 9 (top) shows as well that the *CS-RZ* format has a filter bandwidth penalty of 0.7 dB with respect to *NRZ*, which in turn exhibits a penalty of 0.3 dB only.

Figure 9 (top) also reveals an interesting behaviour in the dependence of the *OSNR* penalty upon the filter bandwidth when using the *33% RZ* format: as it can be seen, a *BER* improvement is measured whenever the filter bandwidth is reduced down to around 0.6 nm. Insets of Fig. 9 (top) show that a quasi *RZ-to-NRZ* conversion is induced by strong optical filtering [25]. This explains the observed performance improvement and the approaching of the *33% RZ* and *NRZ* curves. We believe that under strong optical filtering the *33% RZ* curve would eventually merge with the *NRZ* curve. Unfortunately, we could not narrow down the optical filtering below ~ 0.6 nm owing to the unlocking of our *RZ* clock recovery (based on the recovery of the 40 GHz harmonic in the *RZ* format spectrum).
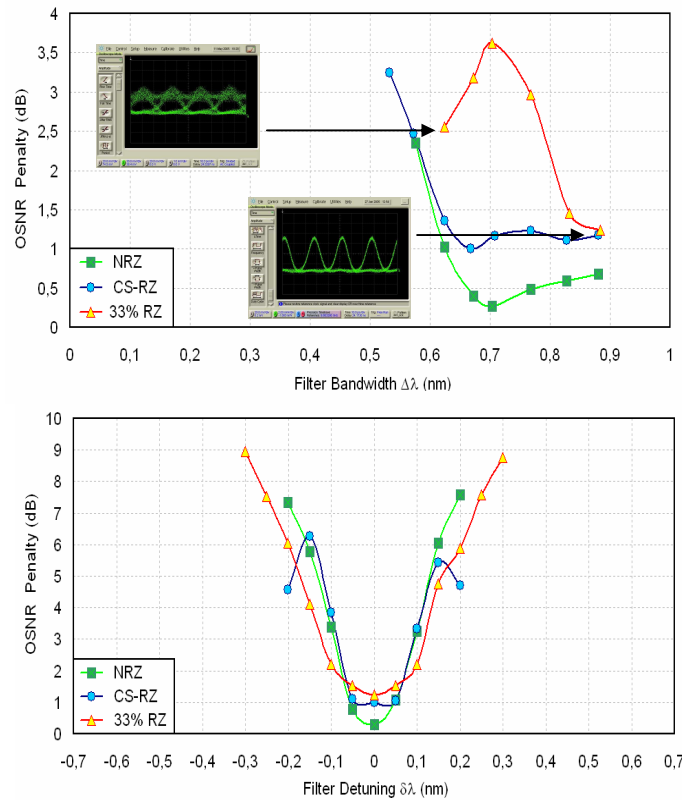

Fig. 9. *OSNR* penalty in 0.5 nm at fixed *BER*=10^{-9} versus the 20-dB filter bandwidth (top) and detuning (bottom), for the central channel at 1550.12 nm. In insets, *33% RZ* eye diagrams when the 20-dB filter bandwidth is set to 0.6 and 0.9 nm.

The modulation format tolerance to output filter detuning is at least as important as the resilience to optical filter bandwidth variations. Figure 9 (bottom) illustrates the observed dependence of the *OSNR* penalty upon optical filter detuning from the channel carrier wavelength. The bandwidth is fixed at its optimal value for each of the formats. As it can be

seen in Fig. 9, the most resistant format to output optical filter detuning is *33% RZ*: the acceptance window (defined here as the filter detuning that introduces a 2 dB penalty) is equal to 0.2 nm for *33% RZ*, and it is equal to 0.15 nm for both *CS-RZ* and *NRZ* formats. The larger the spectral width (and the corresponding optical filter bandwidth), the higher is the modulation format tolerance to optical filter detuning. Whenever a relatively large filter detuning is applied, penalties increase owing to eye diagram distortions and crosstalk from neighbouring channels.

Our measurements compare well with the results of [22] in the particular case of a 100 GHz channel spacing, whenever a rectangular optical filter is employed. For the *NRZ* and *CS-RZ* formats, [22] quotes an optimal optical filter bandwidth of about 90-100 GHz, which is close to our own optimization results.

5. Impact of an OADM cascade on the ASK modulation format performances at 40 Gb/s

To complete the previous study, we have carried out an extensive numerical investigation of the filtering impact of an *OADM* cascade on the performance of our three *ASK* modulation formats [26-28]. We used five channels as in the section 3, but separated now by a spacing of 100 GHz. *VPI Transmission Maker ^{TM}* was still employed with 2048-long *PRBS*. The bandwidth of the square flat-top optical filter located at the receiver was not changed with respect to the optimum value that was found in the previous section. We considered a transmission line consisting of twelve 100-km long *SSMF* fiber spans (17 ps/nm/km, 0.2 dB/km), each of them followed by 16.66 km of dispersion compensation fiber (-100 ps/nm/km, 0.6 dB/km) leading to a 98% compensation ratio (in order to closely match our experimental dispersion map). In contrast with the previous experimental work, we have intentionally extended the length of the transmission line up to 1200 km in order to cascade a sufficient number of *OADM*. The span loss was compensated by a double-stage *EDFA* with 5.5-dB noise figure. The prechirp was still fixed at -850 ps/nm in order to obtain a symmetric dispersion map. The postchirp was optimized in order to obtain the best possible *BER*. The transmitter *OSNR* (measured in 0.5 nm) was kept unchanged for all formats (25 dB). When non-linear effects (*NLE*) were taken into account, we obtained an optimal span input power of 0 dBm per channel. The channel input power in the DCMs was fixed to -2 dBm. The *OADM* were periodically inserted every two spans (corresponding to a total of five *OADM*) and were obtained by the concatenation of an optical 100 GHz demultiplexer (*DEMUX*) and multiplexer (*MUX*). Two types of *MUX / DEMUX* were simulated. The first type had the same characteristics than our *XTRACT* square flat-top optical filter, already used in the receiver. Its amplitude transfer function and group delay response are represented in blue colour on the Fig. 3. As seen on this figure, the 20-dB bandwidth of this filter was close to 100 GHz whereas its peak-to-peak group delay ripple was around 4 ps. The second 100 GHz flat-top *MUX / DEMUX* under study was an ideal one (see the red curves on Fig. 3). The group delay ripple (*GDR*) of this ideal filter was null, whereas its amplitude transfer function was defined by the 1-dB and 20-dB bandwidth, respectively equal to 50 and 145 GHz. Note as well that we have supposed a vanishing insertion loss of the *MUX / DEMUX* at the maximum transmission point. Our results are detailed on the Fig. 10, where the *BER* versus transmission distance was plotted for the *NRZ*, *CS-RZ* and *33% RZ* modulation formats in various configurations (as discussed in the figure legends of Fig. 10 (a-f)).

Let us examine at first the results of Fig. 10(a), where we did not include any fiber nonlinearity nor *OADM*. In this case, we may note that the 100 GHz channel spacing configuration is very detrimental for the *33% RZ* modulation format. The superior resilience of the *33% RZ* format to the accumulation of amplified spontaneous emission (*ASE*) noise, as experimentally observed with the spectral granularity of 200 GHz on the back-to-back plots of the Fig. 6 (bottom), is completely erased when the channel spacing is reduced down to 100 GHz. At the opposite end, Fig. 10(a) shows that the *CS-RZ* format is the most resistant to the accumulation of *ASE* noise: the reduction of the channel spacing to 100 GHz is not sufficient

to remove completely its gain in terms of back-to-back sensitivity observed on the Fig. 6 (bottom) when compared to the *NRZ* format.
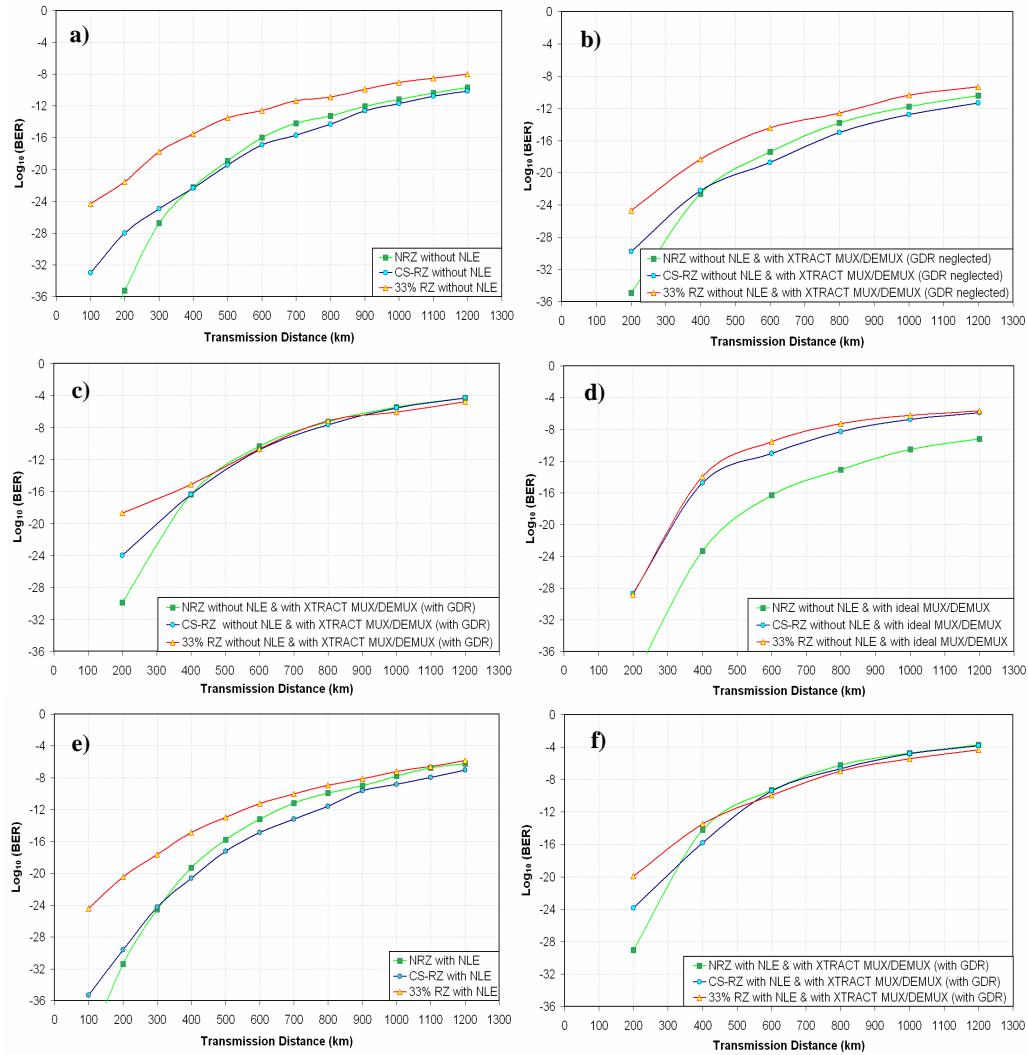

Fig. 10. *BER* versus transmission distance for the *NRZ*, *CS-RZ* and *33% RZ* modulation formats in various configurations: (a) without *NLE* and any *MUX / DEMUX*, (b) without *NLE* but with the *XTRACT MUX / DEMUX* (without GDR), (c) without *NLE* but with the *XTRACT MUX / DEMUX* (with *GDR*), (d) without *NLE* but with the ideal 100 GHz flat-top *MUX / DEMUX*, (e) with *NLE* but without any *MUX / DEMUX*, (f) with *NLE* and with the *XTRACT MUX / DEMUX* (with *GDR*).

Inserting now the *XTRACT MUX / DEMUX* every 200 km while neglecting the *GDR* influence does not degrade the transmission quality at 1200 km as shown in the Fig. 10(b) (this demonstrates that the bandwidth of this *MUX / DEMUX* has been properly chosen). When including the *GDR*, as shown on Fig. 10(c), one obtains a dramatic change of the transmission quality: as it can be seen, the *33% RZ*, *NRZ* and *CS-RZ* formats loose 4.5, 6 and 7 decades on the *BER*, respectively. Therefore the previously observed BER differences among the different formats are virtually erased when GDR is taken into account. Let us consider next replacing the "realistic" *MUX / DEMUX* by the ideal (without *GDR*) 100 GHz flat-top

MUX / DEMUX previously described (see the red curves on Fig. 3). The results of Fig. 10(d) show that the reduced bandwidth (with respect to the *MUX / DEMUX* of Fig. 10(c)) of this ideal filter significantly affects the transmission quality of the *CS-RZ* and *33% RZ* formats (proving that our square flat-top amplitude transfer function with a 20-dB bandwidth of about 100 GHz is more adapted to our system). However, as expected, the *NRZ* format is less affected than the *CS-RZ* and *33% RZ* by the strong optical filtering action of the ideal *MUX / DEMUX*.

The simulation results of Fig. 10(e) show the case where only the nonlinear propagation effects (*NLE*) are taken into account. In this case, by comparing Fig. 10(e) with Fig. 10(a) we notice a general performance degradation. Moreover, nonlinearity leads to an advantage of 1 decade on the *BER* for the *CS-RZ* modulation format at 1200 km when compared to *33% RZ* and *NRZ*. This confirms the results that we already obtained in section 4 when using the spectral granularity of 200 GHz.

Finally, the results of Fig. 10(f) show the performance comparison in the realistic case where the *XTRACT MUX / DEMUX* is inserted each two *SSMF* spans, while its *GDR* as well as the fiber nonlinearity are not neglected. When comparing Fig. 10(f) with the corresponding results of Fig. 10(c), where the *NLE* were not taken into account, we can see that the *BER* is slightly degraded for all modulation formats: at 1200 km, 0.5 and 0.44 decades are lost for the *CS-RZ*, *NRZ* and *33% RZ* formats, respectively. In conclusion, the results of Fig. 10 show that the fine control of the *GDR* of the *OADM* is at least as important in determining the overall system performance as the clever design of the dispersion map, or the precise optimisation of the span input power.

6. Conclusion

Our studies have shown that, although the *33% RZ* format is the most robust to *OSNR* degradation, the CS-*RZ* format is the most tolerant to intra-channel nonlinearities at 40 Gb/s. Both *NRZ* and *CS-RZ* formats exhibit the best tolerance to residual *CD*, whereas *RZ* performs better than *NRZ* and (slightly) *CS-RZ* as far as *DGD* is concerned. Finally, the *NRZ* format is least penalized by filtering, and the *33% RZ* format is the most resistant to filter detuning. As far as the impact of an *OADM* cascade on the transmission quality is concerned, it appears that the *GDR* of the *OADM* has to be precisely controlled in order to limit the overall performance degradation. As expected, modulation formats with large spectral occupancies are most impacted by *OADM* cascades. Overall, from our analysis it appears that using the *CS-RZ* format provides the best balance when trying to meet all different key requirements of future all-optical networks. Nonetheless, due to its relatively poor resilience to *PMD*, the use of the *CS-RZ* format in 40 Gb/s transmission systems is likely to be limited on the existing, high-*PMD* long-haul transport networks. This motivates the current interest in exploring the more complex (and costly) modulation formats such as *DQPSK* [11].

Acknowledgments